Sea Surface Temperature in the Subtropical Pacific Boosted the 2015 El Niño and Hindered the 2016 La Niña

JINGZHI SU

State Key Laboratory of Severe Weather, Chinese Academy of Meteorological Sciences, Beijing, China

RENHE ZHANG

State Key Laboratory of Severe Weather, Chinese Academy of Meteorological Sciences, Beijing, and Institute of Atmospheric Sciences, Fudan University, Shanghai, China

XINYAO RONG

State Key Laboratory of Severe Weather, Chinese Academy of Meteorological Sciences, Beijing, China

QINGYE MIN

Institute of Atmospheric Sciences, Fudan University, Shanghai, China

CONGWEN ZHU

State Key Laboratory of Severe Weather, Chinese Academy of Meteorological Sciences, Beijing, China

(Manuscript received 5 June 2017, in final form 27 October 2017)

ABSTRACT

After the quick decaying of the 2015 super El Niño, the predicted La Niña unexpectedly failed to materialize to the anticipated standard in 2016. Diagnostic analyses, as well as numerical experiments, showed that this ENSO evolution of the 2015 super El Niño and the hindered 2016 La Niña may be essentially caused by sea surface temperature anomalies (SSTAs) in the subtropical Pacific. The self-sustaining SSTAs in the subtropical Pacific tend to weaken the trade winds during boreal spring–summer, leading to anomalous westerlies along the equatorial region over a period of more than one season. Such long-lasting wind anomalies provide an essential requirement for ENSO formation, particularly before a positive Bjerknes feedback is thoroughly built up between the oceanic and atmospheric states. Besides the 2015 super El Niño and the hindered La Niña in 2016, there were several other El Niño and La Niña events that cannot be explained only by the oceanic heat content in the equatorial Pacific. However, the questions related to those eccentric El Niño and La Niña events can be well explained by suitable SSTAs in the subtropical Pacific. Thus, the leading SSTAs in the subtropical Pacific can be treated as an independent indicator for ENSO prediction, on the basis of the oceanic heat content inherent in the equatorial region. Because ENSO events have become more uncertain under the background of global warming and the Pacific decadal oscillation during recent decades, thorough investigation of the role of the subtropical Pacific in ENSO formation is urgently needed.

1. Introduction

As the most prominent interannual variability in the tropical Pacific, El Niño–Southern Oscillation (ENSO) exerts significant climate influences in many regions worldwide. Scientists have focused on the mechanisms involved in ENSO and have attempted to predict ENSO events with a lead time of 1 year or more (McPhaden et al. 1998; Latif et al. 1998; Barnston et al. 2012). Generally, there are two prerequisites for an El Niño event: anomalous warm waters accumulating in the equatorial Pacific (e.g., Wyrtki 1985; Chen et al. 2016) and the presence of westerly wind events (WWEs) (e.g., Luther et al. 1983;

Denotes content that is immediately available upon publication as open access.

Corresponding author: Dr. Su Jingzhi, sujz@cma.gov.cn

DOI: 10.1175/JCLI-D-17-0379.1

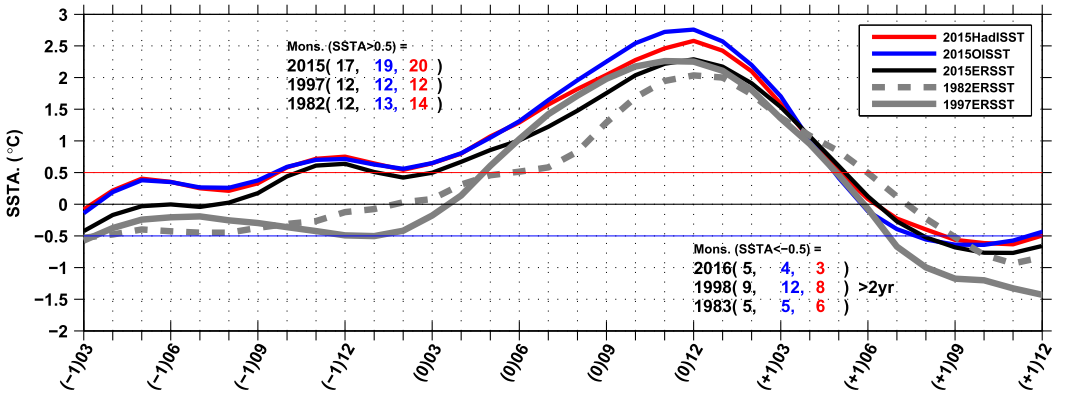

FIG. 1. The SSTA time series averaged in the Niño-3.4 region (5°N–5°S, 120°–170°W) for the El Niño events of 1982 (gray dashed), 1997 (gray solid), and 2015 (black, blue, and red solid). The SSTA time series are smoothed with a 3-month running mean, as per the definition of the ONI. For each El Niño event, the number of months meeting the threshold of ±0.5°C for the warm/cold status are shown for the results obtained based on ERSST, OISST, and HadISST as black, blue, and red text, respectively.

McPhaden et al. 1992; D. Chen et al. 2015). When such conditions coincide, anomalously warm waters can be readily transported eastward by anomalous oceanic currents (e.g., McPhaden and Picaut 1990) or propagate eastward as downwelling Kelvin waves (e.g., Wyrtki 1975; Miller et al. 1988; Huang et al. 2001), causing anomalous warming in the central-eastern equatorial Pacific. Such conceptual models have been verified in practical predictions for almost all El Niño events.

However, ENSO predictions have encountered unexpected challenges in recent years. In the boreal summer of 2012, an El Niño event was predicted to arise in the subsequent seasons. However, the already warmed ocean in the eastern equatorial Pacific suddenly reversed back to a neutral condition in September 2012 (Su et al. 2014b). A similar event also occurred in the boreal summer of 2014 (Min et al. 2015; Zhu et al. 2016; Hu and Fedorov 2016). An exceptionally strong El Niño event was predicted and discussed in public media in the beginning of 2014. However, the rapid growth of the anomalous warming in the central-eastern equatorial Pacific dramatically paused during the summer, and no El Niño event formed until the end of 2014 (http://www.cpc.ncep.noaa.gov/products/analysis_monitoring/enso_disc_dec2014/ensodisc.html). Since April 2016, the National Oceanic and Atmospheric Administration (NOAA)'s Climate Prediction Center (CPC) repeatedly announced that a La Niña event would occur during the following winter. However, this La Niña event failed to reach an expected magnitude, with a short lifetime (Fig. 1; http://www.cpc.ncep.noaa.gov/products/analysis_monitoring/enso_disc_dec2016/ensodisc.pdf). These failures in ENSO prediction remind us that present conceptual models of ENSO remain incomplete and need careful inspection.

The tough challenge in prediction for the several past ENSO events can be attributed to the ENSO diversity during recent decades. For example, more and more El Niño events showed spatial patterns centered in the central Pacific (CP) after 2000, different from those classical El Niño events centered in the eastern Pacific (EP; e.g., Ashok et al. 2007). The different flavors of EP-type El Niño and CP-type El Niño may be led by the diversity of westerly wind bursts (Hu et al. 2014; D. Chen et al. 2015; Fedorov et al. 2015). From another aspect, the sea surface temperature anomalies (SSTAs) in the subtropical Pacific can persist from boreal winter to summer and affect ENSO development in the central-eastern equatorial Pacific (Vimont et al. 2003; Yu et al. 2010). Furthermore, certain SSTAs in the subtropical Pacific may also contribute to the formation of different types of El Niño (Zhang et al. 2014; Min et al. 2017). Cooling SSTAs in the subtropical Pacific may have acted as a key factor in hindering El Niño development in 2012 and 2014 (Su et al. 2014b; Min et al. 2015; Zhu et al. 2016). It also was shown that some episodes of easterly wind surge during the summer of 2014 might directly hinder the El Niño development (Menkes et al. 2014; Hu and Fedorov 2016). Wu et al. (2018) suggested that the meridional SSTAs gradient was reinforced by the cold SSTAs in the eastern South Pacific and the warm SSTAs in the eastern North Pacific, and then induced surface cross-equatorial flow, which ultimately suppressed the 2014 El Niño development.

After the hindered 2014 El Niño, the western Pacific warm pool extended eastward and warmer SSTAs persisted near the central equatorial Pacific in the beginning

of 2015, which provided a favorable precondition for the strong El Niño in 2015 (Hu and Fedorov 2018). Subsequently, some strong WWEs pushed the 2015 El Niño into a substantial development phase (Xue and Kumar 2017; Hu and Fedorov 2018; Chen et al. 2017). Compared with the 1997 El Niño, the 2015 El Niño was blended with some characters of CP-type El Niño, which was probably brought by the warm SSTAs in the subtropical Pacific, and the subtropical warm SSTAs could also lead a slow decay of this El Niño in 2016 (Paek et al. 2017).

As mentioned by several previous papers, the strong WWEs played an essential role in the development of the 2015 super El Niño, and the ENSO diversity may be caused by the variation in WWEs. Hence, the fundamental mechanism for the generation of those strong WWEs in 2015 should be investigated in details. Furthermore, the 2015 El Niño prolonged for more than one and half years (Fig. 1), ranked as the longest one among the several strongest El Niño events. Generally, a strong El Niño event (e.g., 1982/83 and 1997/98) was followed by a long-lasting La Niña event (Fig. 1). However, the La Niña following the 2015 strong El Niño was unexpectedly hindered during the boreal summer of 2016. This study will investigate the development processes of the 2015 El Niño and hindered La Niña in 2016 as a whole, with a focus on the important influences exerted by different SSTA patterns in the subtropical Pacific. Furthermore, we also try to generalize the role of SSTAs in the subtropical Pacific in El Niño and La Niña development, using some statistical analyses and model simulations.

The data and experiments are described in section 2. The observed results about 2015 El Niño and 2016 La Niña are given in section 3. Experiment results are shown in section 4. Section 5 investigates the processes of the subtropical Pacific forcing on ENSO. In section 6, more ENSO events are described to show the role of the subtropical Pacific, and its decadal changes are described in section 7. A summary and discussion are provided in section 8.

2. Data and experiments

The SST fields were obtained from the Extended Reconstructed Sea Surface Temperature SST, version 4 (ERSST.v4) with a resolution of 2° × 2° (Huang et al. 2015), the NOAA Optimum Interpolation Sea Surface Temperature, version 2 (OISSTv2) with a resolution of 1° × 1° (Reynolds et al. 2002), and the Hadley Centre Sea Ice and Sea Surface Temperature dataset, version 1 (HadISST1), with a resolution of 1° × 1° (Rayner et al. 2003). The precipitation fields were from the CPC Merged Analysis of Precipitation (CMAP) with a resolution of 2.5° × 2.5° (Xie and Arkin 1997). The surface wind stress and 10-m wind data were obtained from the European Centre for Medium-Range Weather Forecasts (ECMWF) interim reanalysis (ERA-Interim) with a resolution of 1.125° × 1.125° (Dee et al. 2011). The oceanic temperature and currents were provided by the National Centers for Environmental Prediction (NCEP) Global Ocean Data Assimilation System (GODAS) with a horizontal resolution of 1° longitude and 1/3° latitude, and a vertical resolution of 10 m for the upper 200 m (Saha et al. 2006). The thermocline depth values are calculated as the 20°C isotherm based on the GODAS dataset. All the analyses were performed based on the time period of 1980–2016 for all data, and the climatological annual cycle is calculated based on the period of 1981–2010 in this study.

The sensitivity experiments were carried out based on the atmospheric general circulation model of ECMWF Hamburg Model (ECHAM) version 5.4 (ECHAM5.4; Roeckner et al. 2003), with a horizontal spectral resolution of T63 and 19 vertical levels (T63L19). The SST fields used to force the model were derived from the OISST monthly datasets. A 50-yr model control run was forced continually by the climatology of SST fields. The restart files on 1 January obtained from the control run are used as initial conditions for sensitivity runs. Each type of sensitivity run is composited of an ensemble of 20 members. Each member of the sensitivity runs was integrated for 12 months from 1 January with different initial conditions obtained from the last 20 years of control run. Then the average of all the values simulated by the 20 members in sensitivity runs is used to be compared with that simulated by control run, and the differences are shown and discussed in the following. In the sensitivity runs, the model was forced by the composites of climatological SST fields and the prescribed 2015 SSTA fields in different regions. Overall, six types of sensitivity runs were designed in this study. First, in the global run, the prescribed 2015 SSTAs were applied to the global ocean grids. Then in the other five runs, the 2015 SSTAs were prescribed only on grids in some specific regions (e.g., Pacific region), and the remaining regions were set to climatological SST. The details of regions with prescribed SSTAs for the six designed experiments are shown in Table 1. The sea ice fields were set to climatological values for both control run and sensitivity runs.

3. Observational results

a. *The evolution of the super El Niño in 2015*

Although the El Niño was hindered during the boreal summer in 2014, the SSTAs in the Niño-3.4 region (5°N–5°S, 120°–170°W) warmed gradually after August and

TABLE 1. The boundary of designed regions with prescribed 2015 SSTAs that are superimposed on the climatological SST fields in each experiment. The eastern boundary is the west coast of the Americas. The rest regions are set with climatological SST fields.

Experiment	Abbreviation	North–south extent	Western boundary
Global	Glb	90°S–90°N	None
Pacific	Pac	55°S–55°N	120°E, including the South China Sea
Equatorial Pacific	EQPac	5°S–5°N	120°E
Subtropical Pacific	STPac	55°–5°S and 5°N–50°N	120°E
Northeastern Pacific	NESTPac	5°N–50°N	180°
Southeastern Pacific	SESTPac	55°–5°S	180°

reached above 0.5°C after October 2014 (Fig. 1). Since then, the Niño-3.4 SSTA primarily kept above 0.5°C until the 2015/16 El Niño decayed around May 2016. As a result, the 2015 El Niño persisted for about one and a half years, much longer than the 1982 El Niño and the 1997 El Niño (about one year).

Starting from a high point of warm water accumulated in 2014, a persistent rise of the positive SSTAs in Niño-3.4 appeared in February 2015 (Fig. 1). In February 2015, warm water began to emerge around 180°, associated with strong WWEs over the western Pacific (around 120°E–180°), and then extended eastward to the eastern equatorial Pacific (around 130°–80°W; Fig. 2c). The initial warming status prior to March 2015 shared similarities with conditions in 1997 (Fig. 2a) and 2014 (Fig. 2b). The bifurcation of the initial similar status in 2014 and 2015 started approximately in April. The WWEs gradually diminished after March 2014, and some strong anomalous easterlies (Min et al. 2015), namely easterly wind events (Hu and Fedorov 2016), showed up in the central-eastern equatorial Pacific during the boreal summer of 2014. On the other hand, the strong WWEs were enhanced after April 2015 and extended eastward rapidly. Subsequently, the strong westerly anomalies in 2015 occupied the region from the western Pacific to the central-eastern equatorial Pacific (around 180°–80°W), a large area comparable to that in 1997.

The persistence and enhancement of the WWEs in 2015 was associated with extra warming in the subtropical North Pacific (SNP). During the summer of 2015, significant positive SSTAs (>1.0°C) persisted in the SNP (Fig. 3c), which favored anomalous convection there and caused a cyclonic surface wind pattern near the SNP, as a Gill-type Rossby wave response (Gill 1980). Correspondingly, the trade winds were weakened in the North Pacific, with anomalous southwesterlies between the equator and 15°N. At the same time, there was also another anomalous convective center along the equator, because of the already warming in the central-eastern equatorial Pacific. The coexistence of the anomalous convective center at the equator and the one at the SNP can be demonstrated by a wide meridional

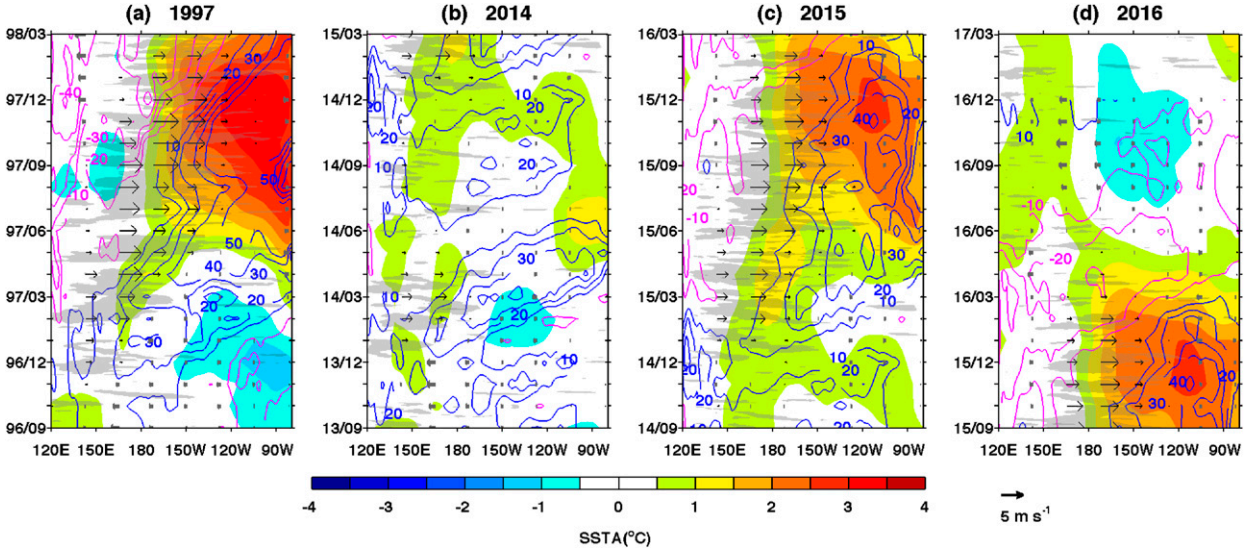

FIG. 2. The SSTAs (shading) from the ERSST.v4 dataset, thermocline depth anomalies (contour lines; negative values with magenta lines and positive values with blue lines, with intervals of 10 m) from the GODAS, and anomalous zonal wind at a height of 10 m (vector; m s^{-1}; eastward anomalies with black thin lines and westward anomalies in gray thick lines) along the equator (within 5°N–5°S) are shown for (a) 1997, (b) 2014, (c) 2015, and (d) 2016. The gray shaded patches indicate the periods with daily zonal wind anomalies larger than 2 m s^{-1}, roughly representing the episodes of westerly wind events. The zonal winds are derived from ERA-Interim, and daily values are smoothed with a 3-day running mean.

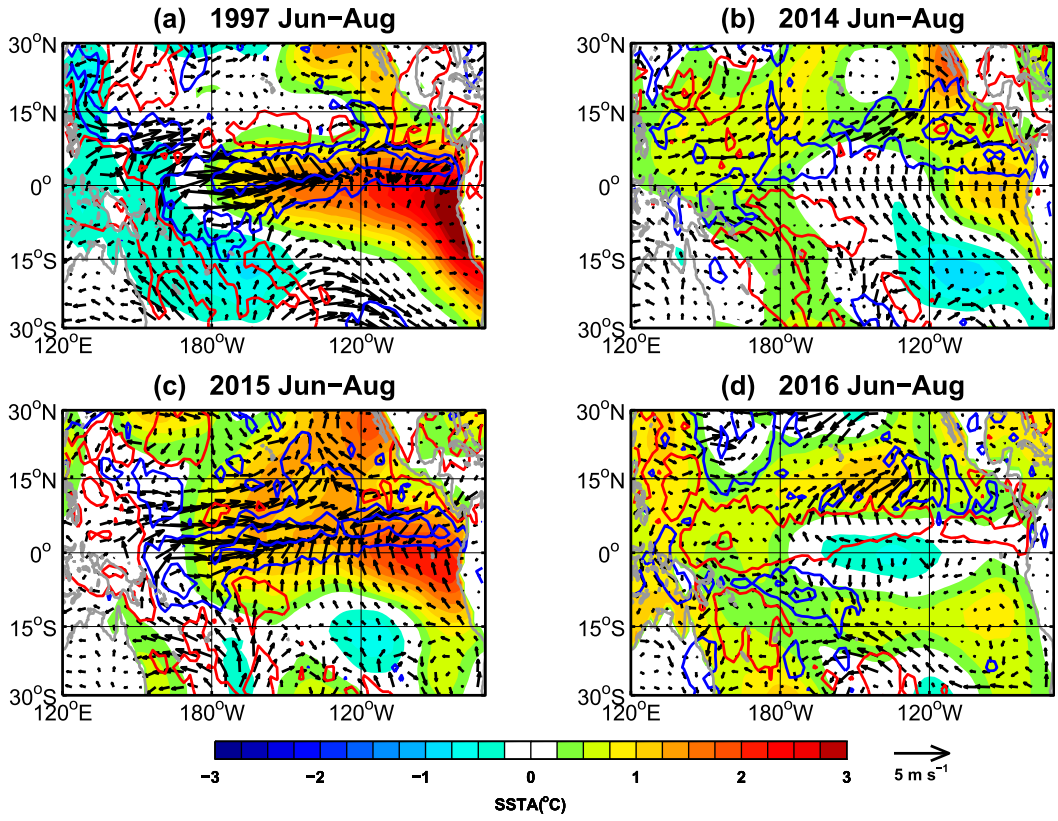

FIG. 3. SSTAs (shading, with intervals of 0.25°C), anomalous precipitation (contours of ±1 and ±5 mm day^{-1}, blue for positive and red for negative), and anomalous wind at a height of 10 m (vector; m s^{-1}) during June–August of (a) 1997, (b) 2014, (c) 2015, and (d) 2016. The wind, precipitation, and SST data were obtained from ERA-Interim, GPCP, and ERSST, respectively.

extension of the precipitation anomalies in the region of 150°–120°W (Fig. 3c). Such an anomalous convection center in the SNP was absent in the case of the 1997 El Niño, during which the precipitation anomalies were primarily confined within the equatorial region (Fig. 3a). These anomalous southwesterlies north of the equator during the summer of 2015, which were directly related to the positive SNP SSTAs, gradually merged with those equatorial westerly anomalies in the western-central Pacific (around 120°E–130°W), enhancing the westerly anomalies along the equator there. Hence, the weakened trade winds in the SNP (i.e., the anomalous westerlies north of the equator), might have played an important role in maintaining strong WWEs in the western-central equatorial Pacific, a key factor for El Niño development in 2015. It was also demonstrated that the warming SSTAs in subtropical Pacific favored an atypical Madden–Julian oscillation, as well as the persistent WWEs, followed by the onset of the 2015/16 El Niño (Hong et al. 2017).

Such persistent strong westerly anomalies were absent in 2014 (Fig. 2b). The trade winds were enhanced south of the equator in 2014, caused by extreme cooling in the subtropical South Pacific (SSP; 10°–20°S, 130°–90°W) (Fig. 3b; Min et al. 2015). As an extension of the enhanced trade winds, anomalous easterlies developed in the central equatorial Pacific, hindering the formation of El Niño in 2014, which was also confirmed by the studies of Hu and Fedorov (2016). The extreme cold SSTAs in the SSP gradually faded away after 2014. Both the amplitude and the spatial extension of the cold SSTAs in the SSP in 2015 were apparently weaker than those in 2014. As a result, the trade wind anomalies south of the equator in 2015 were quite different from those in 2014, with almost zero zonal components in the central Pacific during the summer of 2015 (Figs. 3b,c). In addition, positive SSTAs in the SNP reached a higher value above 1.0°C in 2015 than that in 2014 (<0.5°C; Figs. 3b,c), which caused a greater weakening of the trade winds north of the equator in 2015. As a result, positive SSTAs in the SNP boosted El Niño development in 2015, whereas the negative SSTAs in the SSP hindered El Niño growth in 2014.

The role of the SNP in the formation of the 2015 El Niño can be further highlighted by comparison with

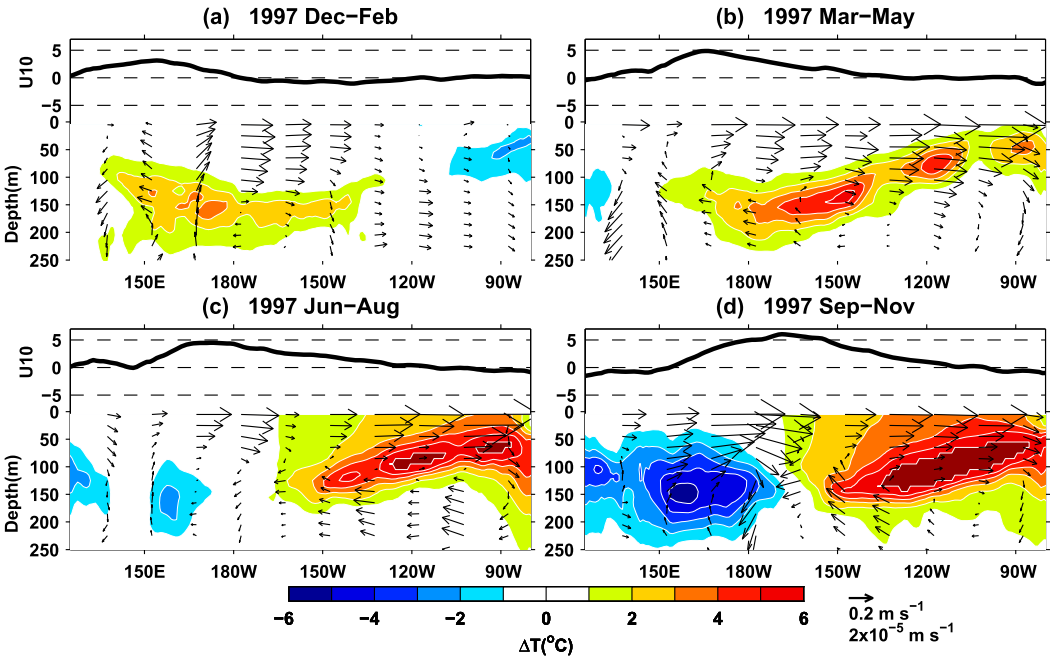

FIG. 4. Composite anomalies zonal wind at a height of 10 m (black lines at top; m s^{-1}), oceanic temperature anomalies (color shading; °C), and oceanic current anomalies (vectors; m s^{-1}) along the equator (within 5°N–5°S) during each season in 1997. The oceanic data are from GODAS. The wind data are from ERA-Interim.

the 1997 El Niño. Significant positive subsurface anomalies accumulated in the western-central Pacific at the beginning of 1997 (Fig. 4a), which is a good indicator for the formation of an El Niño event. However, positive subsurface temperature anomalies in the western-central Pacific were much weaker in the beginning of 2015 than those in 1997 (Fig. 5a). Only after February 2015 did significant positive subsurface anomalies begin to emerge around 180° under the forcing of strong WWEs (Fig. 5b). These features were also described by Paek et al. (2017) and Chen et al. (2017). An anomalous cyclonic wind pattern formed in the location north of the anomalous westerly in the western Pacific after February 2015 (not shown, but can be inferred from Fig. 3c). The cyclonic wind anomalies then induced upwelling in the upper ocean and caused cold subsurface anomalies in the western Pacific (Fig. 5b), similar to the corresponding essential link in the delayed oscillator for ENSO (Suarez and Schopf 1988).

b. *The hindered La Niña in 2016*

The SSTAs in the Niño-3.4 region faded quickly after its peak in December 2015, reaching a neutral state after April 2016 (Figs. 1 and 2d; Paek et al. 2017). A La Niña event was repeatedly predicted during April–November 2016 by the CPC (http://www.cpc.ncep.noaa.gov/products/expert_assessment/ENSO_DD_archive.shtml). However, the SSTAs in the central-eastern equatorial Pacific maintained a negative state with a relatively weak amplitude (around −0.6°C) for the five months during July–November 2016 (Figs. 1 and 2d). The negative SSTA state in 2016 failed to transform into a full-fledged La Niña event, based on the threshold of a period of at least five consecutive overlapping 3-month seasons with an oceanic Niño index (ONI) below −0.5°C. The ONI is defined as 3-month running mean of SSTA in the Niño-3.4 region. In fact, a weak La Niña event in 2016 can be obtained only based on a single dataset, ERSST.v4; other SST datasets (e.g., OISST and HadISST) showed a neutral ENSO status in 2016.

This failure of the negative Niño-3.4 SSTA to evolve into a matured La Niña event in 2016 can be attributed to the warm SSTAs in the SNP and the SSP (Fig. 3d). The warm subtropical SSTAs induced anomalous convection centers in both the North Pacific (around 13°N, 130°W) and the South Pacific (around 12°S, 170°W), indicated by positive precipitation anomalies there (Fig. 3d). Consequently, the trade winds were weakened on both sides of the equator, which further prevented the enhancement of anomalous easterlies near the equator. As a result, although the Niño-3.4 SSTA once dropped almost to −1°C around October 2016, no significant anomalous easterlies along the western-central equator

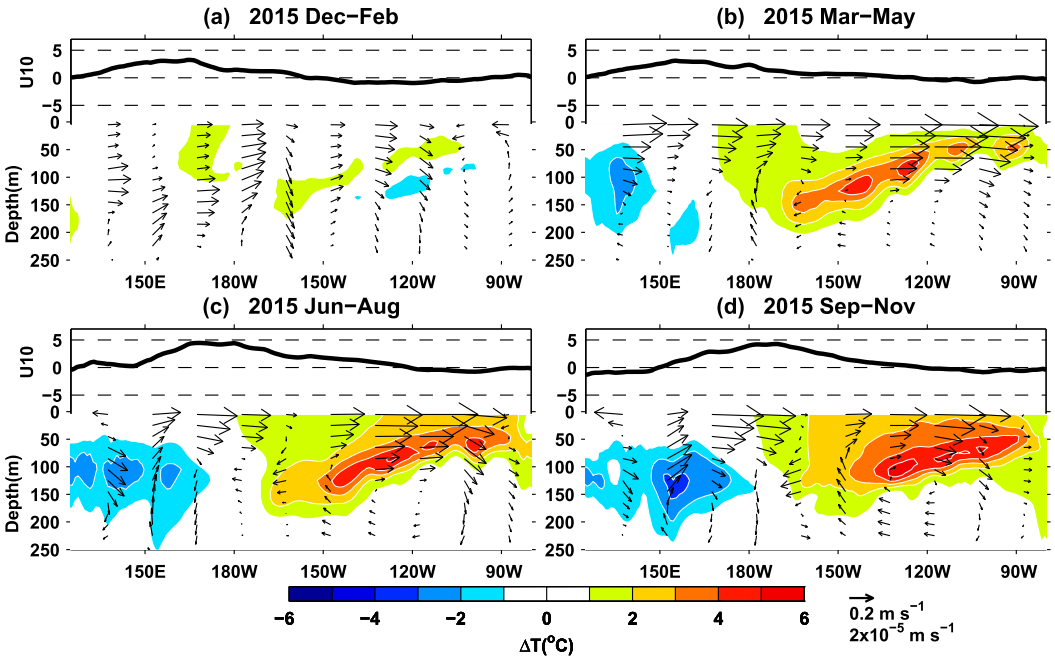

FIG. 5. As in Fig. 4, but for 2015.

(around 130°E–130°W) were observed during most of 2016 (Figs. 2d and 3d).

4. Results of numerical experiments

To investigate the potential role of the SSTAs in the subtropical Pacific with regard to the zonal wind variabilities along the equator, some numerical experiments were performed using an atmospheric general model of ECHAM5.4. Forced by the global observed SSTAs in 2015 (Glb), strong anomalous westerlies in the western equatorial Pacific can be well simulated during the boreal summer, with enhanced precipitation around the central equatorial Pacific (Fig. 6a). Such patterns of surface winds and precipitation anomalies are also captured by simulations with prescribed SSTAs only in the Pacific (Pac; Fig. 6b). If the prescribed SSTAs are confined to the subtropical Pacific (STPac; Fig. 6d)—that is, omitting the equatorial region within 5°N–5°S—the simulated atmospheric responses are different from those forced only by SSTAs in equatorial Pacific (EQPac; Fig. 6c). The enhanced precipitation center is located in the western-central equatorial region if forced only by the SSTAs in the equatorial Pacific (Fig. 6c). On the other hand, the enhanced precipitation center moves northeastward to the region around 15°N, 130°W, close to the warming center in the subtropical North Pacific in the STPac experiment (Fig. 6d). Further experiments show that anomalous convection is more readily generated under the forcing of warm subtropical SSTAs in the northeastern Pacific (NESTPac; Fig. 6e) than in the southeastern Pacific (SESTPac; Fig. 6f), as the observed 2015 SSTAs in the northeastern Pacific were warmer than those in the southeastern Pacific. One reason for convection anomalies to be readily formed in the northeastern Pacific is that a warm pool is located in the northeastern Pacific, as a threshold of about 27.5°C is usually required for the generation of deep convective activity (Graham and Barnett 1987).

Based the comparison between the results of the above experiments, it can be demonstrated that the warm SSTAs in the subtropical North Pacific can readily induce anomalous convection centered at off-equatorial latitudes, forming a Gill-type Rossby wave pattern near the warming center. Associated with the off-equatorial cyclonic atmospheric response, the trade winds are weakened and anomalous southwesterlies are formed near the equator. Such southwesterly anomalies can extend to the equator and then enhance the anomalous westerlies along the equator (Fig. 7). Particularly, if forced by the SSTAs prescribed only within the equatorial region, the induced westerly anomalies in the western Pacific cannot extend to the Niño-3.4 region. On the other hand, the warm SSTAs in the subtropical northeastern Pacific can favor anomalous westerlies with a large zonal extension, covering the Niño-3.4 region, which is a key factor for the maintaining the warming SSTA tendency

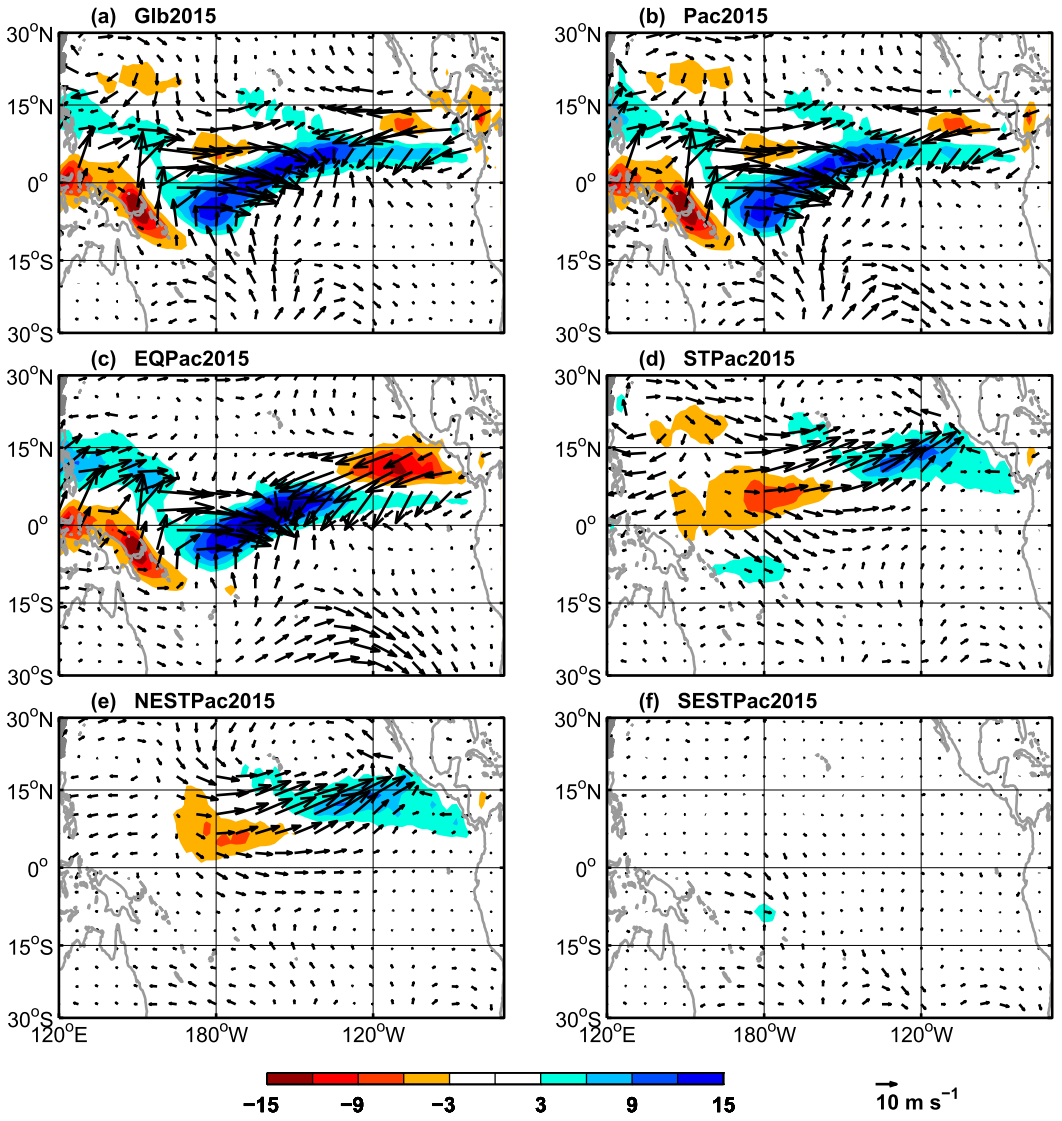

FIG. 6. The wind anomalies at a height of 10 m (vector; m s^{-1}) and precipitation anomalies (shading; mm day^{-1}) simulated by the ECHAM. The values shown are difference between the average of the 20 members for each sensitivity experiment and the corresponding values in the control experiment. The 2015 SSTAs are prescribed in (a) the global ocean, (b) the Pacific, (c) the equatorial Pacific, (d) the subtropical Pacific, (e) the northeastern Pacific, and (f) the southeastern Pacific (see Table 1).

locally by favoring the formation of positive Bjerknes feedback.

5. The processes during the subtropical Pacific forcing on ENSO

The important influences of the subtropical Pacific on ENSO formation can be further confirmed by general analyses in addition to the above case analyses. The lead–lag correlation analyses (Fig. 8a) show that subtropical Pacific SSTAs during the leading period of March–July [MAMJJ; i.e., Mar(0)–Jul(0), where 0 indicates the year of the event] can favor ENSO formation during the following autumn–winter season, represented by the SSTAs in the Niño-3.4 region during the period of October–February [Oct(0)–Feb(+1), where +1 indicates the following year]. As the subtropical Pacific can be influenced by the leading/synchronous equatorial SSTAs through atmospheric bridge (Alexander et al. 2002), the lead–lag correlations are further performed based on the SSTA fields in which the linear least squares fit to the 1-month leading SSTA in Niño-3.4 was subtracted (Fig. 8b). A robust relationship can be found between the previous spring–summer

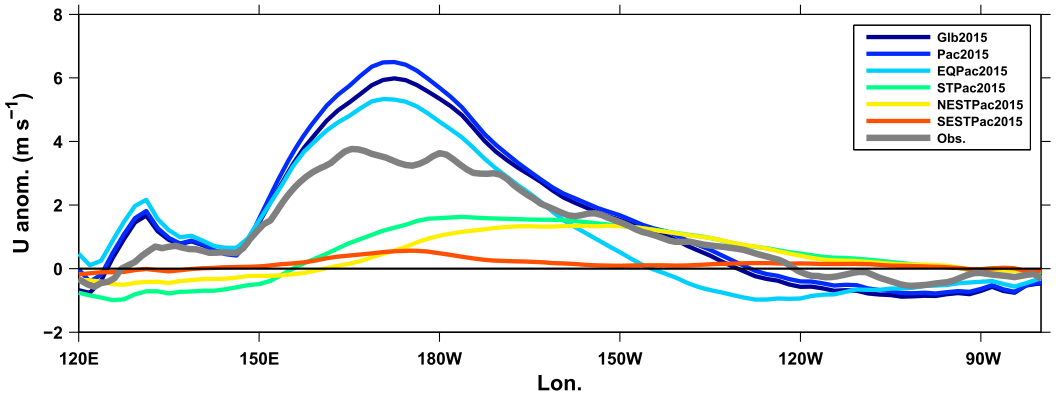

FIG. 7. The observed (thick gray) and simulated zonal wind anomalies at a height of 10 m (m s^{-1}) along the equator (within 5°N–5°S) by ECHAM for each sensitivity experiment. The values shown are difference between the average of the 20 members for each sensitivity experiment and the corresponding values in the control experiment.

SSTAs in the subtropical North Pacific and the following ENSO formation, in both schemes of correlation calculation.

To perform further statistical analysis about the influence of subtropical Pacific on El Niño and La Niña formation, two regions are chosen here to represent the subtropical Pacific. For the subtropical North Pacific, the region is defined as the SNP (5°–15°N, 140°–170°W), where the MAMJJ SSTAs have significantly high correlation with later Niño-3.4 index. For the subtropical South Pacific, we selected a region of the SSP (10°–20°S, 130°–90°W), following the definition of Min et al. (2015). The SSP is located near the main center of the South Pacific meridional mode [see Fig. 2b in Min et al. (2017)]. The SSTAs in the SSP have a large interannual variability and can capture the extreme cooling in 2014 and the extreme warming in 2016 (Fig. 9b).

It should be noted that the SSTAs in the subtropical Pacific during the spring–summer can be maintained or enhanced by the wind–evaporation–SST (WES) mechanism (Xie and Philander 1994). Although significant warming has prevailed in the far northeastern Pacific for several years since around 2013 (Di Lorenzo and Mantua 2016), the SSTAs in the region of SNP began to rise up to above 0.5°C only after January 2015 (Fig. 9a). The SNP SSTAs gradually increased during the spring–summer of 2015, with positive latent heat fluxes imposed into the ocean during the same time (Fig. 9a), following the WES mechanism. Following Su et al. (2010), a heat budget analysis was performed for the upper mixed layer temperature in the SNP, using the oceanic variables from GODAS data and the composited values of surface heat flux from ERA-Interim, NCEP-1, NCEP-2, and OAFlux. It was showed that heat convergence by

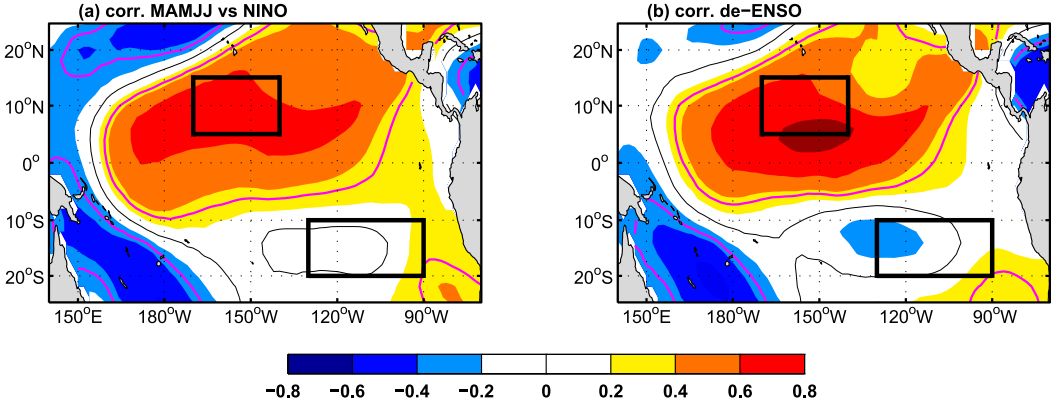

FIG. 8. (a) Correlations between the SSTA during Mar(0)–Jul(0) and the Niño-3.4 index during the period of Oct (0)–Feb(+1). (b) As in (a), but the linear least squares fit to the 1-month leading Niño-3.4 index was subtracted before the calculation. The magenta lines indicate regions significant at the 95% confidence level. The thick black boxes indicate the defined regions of the subtropical North Pacific (5°N–15°N, 140°–170°W) and the subtropical South Pacific (10°–20°S, 130°–90°W) as used in statistical analyses.

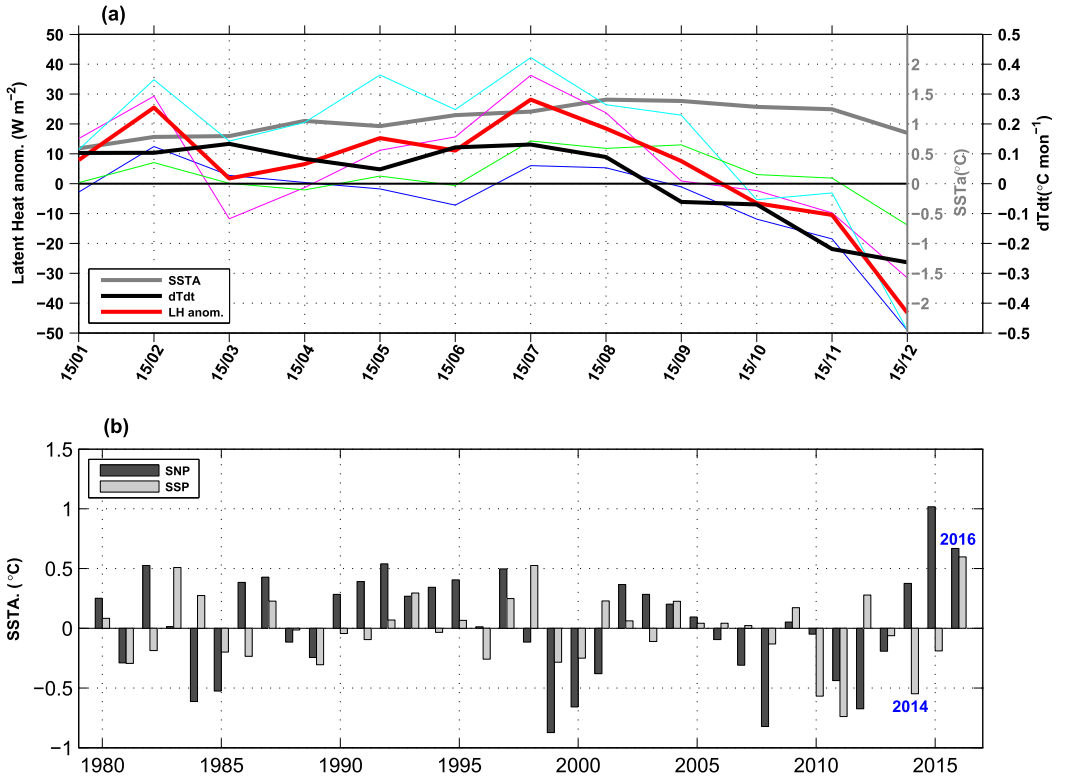

FIG. 9. (a) The mean latent heat flux anomalies (red), SSTA (gray), and time tendency (black) of SSTA time series averaged in the SNP region (5°–15°N, 140°–170°W). The latent heat flux anomalies derived from ERA-Interim (blue), NCEP-1 (magenta), NCEP-2 (cyan), and OAFlux (green) are shown with thin lines. The latent heat flux values are positive downward. (b) The mean SSTA during MAMJJ averaged in the SNP and the SSP region (10°–20°S, 130°–90°W) for each year.

the oceanic dynamic processes was negative during MAMJJ in 2015. The observed positive tendency of SSTAs in SNP (0.08°C month^{-1}) was mainly contributed by the surface heat flux anomalies (0.11°C month^{-1}), and the term of downward latent heat flux anomalies was the major contributor (0.12°C month^{-1}).

Associated with the self maintenance of the SNP SSTAs, the trade winds were weakened during the spring–summer of 2015, indicated by the northeastward wind anomalies north of the equator (Fig. 10b). Before June 2015, the horizontal spatial pattern of the winds anomalies matches the Pacific meridional mode (e.g., Min et al. 2017), with anomalous meridional winds flowing from the cold SSTAs in the South Pacific to the warm SSTAs in the North Pacific (Fig. 10b). The anomalous westerlies were mainly located on the north side of the equator in the central-eastern Pacific. On the equator, however, the wind anomalies have a very weak zonal component. Furthermore, the precipitation anomalies were also located north of the equator, about between 5° and 10°N. In the case of 1997 El Niño, the anomalous westerlies, as well as the anomalous convection, mainly located near the equator (Fig. 10a). Hence, we can conclude that the convection anomalies, as well as the anomalous westerlies, in the central Pacific were primarily induced by the warm SSTA in SNP before June 2015. Since June 2015, the SSTA around the Niño-3.4 warmed up to about 1°C. Consequently, the anomalous precipitation center moved toward to the equator. At the same time, the wind anomalies near the equator were generally zonal westerlies, pointing to the eastern warm SSTAs in the equatorial region. Those features indicated that the SSTAs in Niño regions, from then on, started to work as an active factor, forming a positive Bjerknes feedback between the atmospheric activities.

Here, we want to focus on the role of the subtropical SSTAs to maintain the anomalous westerlies on seasonal time scales, before an effective Bjerknes feedback is really set up over the equatorial regions. After the SSTAs in the Niño regions are warmed enough, the convection anomalies near the equator work as a primary driver for the tropical atmospheric circulation. After then, the trade winds can be weakened further under the influence of equatorial convection anomalies.

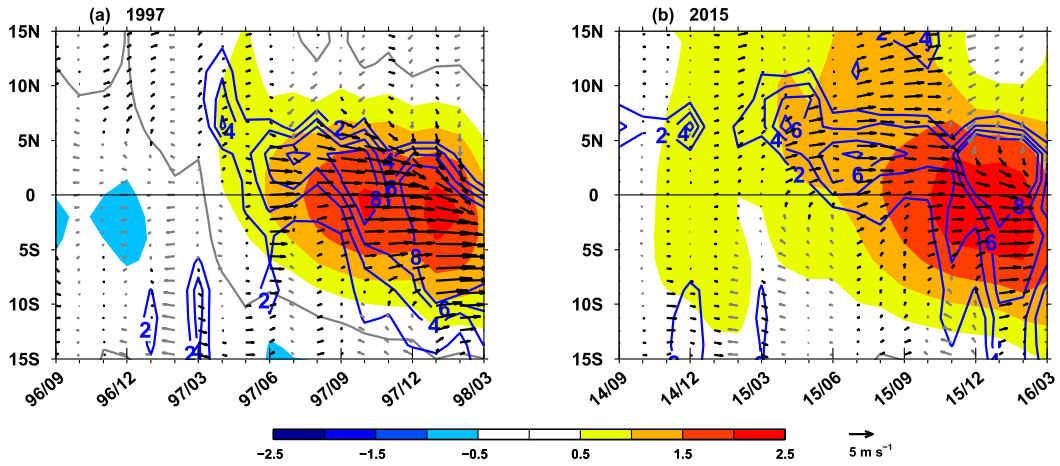

FIG. 10. The SSTAs (shading; gray contours are zero), positive precipitation anomalies (blue contours, with intervals of 2 mm day^{-1}), and zonal average of anomalous wind at a height of 10 m (vector; m s^{-1}; eastward anomalies with black vectors and westward anomalies in gray vectors) along the central Pacific (180°–130°W) for (a) 1997 and (b) 2015.

In short, it is logical to investigate the influence of the subtropical Pacific on ENSO formation in two steps, separately. In the first step, before an effective Bjerknes feedback is formed over the equatorial regions, the subtropical SSTAs play an active role to induce changes of trade winds. In the second step, when the El Niño event essentially comes into being, the equatorial convection anomalies also favor the trade winds changes.

6. More cases to show the role of subtropical Pacific

The correlation between the SNP SSTAs during Mar(0)–Jul(0) and the SSTAs in Niño-3.4 during Oct(0)–Feb(+1) reaches 0.64, significant at the 95% confidence level. The scatterplot in Fig. 11a shows that the positive SNP SSTAs are quite often the precursor of El Niño events, while the La Niña events are usually led by negative SNP SSTA. For the subtropical South Pacific, the leading SSP SSTAs have a poor correlation (corr = 0.02) with the winter ONI (Fig. 11b). However, in some particular ENSO events (Table 2) the effects of SSP SSTAs on the following winter ONI were as salient as those of the SNP SSTAs, as discussed below. As it is well recognized that the upper ocean heat content, or the warm water volume (WWV), of the equatorial Pacific can act as a good indicator of ENSO prediction (e.g., Meinen and McPhaden 2000; McPhaden 2012), comparisons between the WWV and the SNP/SSP SSTAs are given to clarify the role of the subtropical Pacific on ENSO formation. The WWV is represented by the thermocline depth anomalies (Z20) averaged within 5°N–5°S. Besides the basinwide WWV of the equatorial Pacific (120°E–80°W), the WWV of the western Pacific (120°E–180°) is also shown, as the latter was also shown to have important effects on ENSO development (e.g., Chen et al. 2016). The low correlation (corr = −0.02) between the SNP SSTA and the basinwide WWV during the same period of Mar(0)–Jul(0) indicates that the leading SNP SSTA can be treated as an independent indicator for ENSO prediction. On the other hand, the SNP SSTA seems highly correlated with the WWV in western Pacific during the same period of Mar(0)–Jul(0) (corr = −0.62), as they are both directly related to the Pacific decadal oscillation (PDO).

For the 2015 super El Niño, the tropical ocean provided a WWV precondition of only moderate strength, ranking eighth among all the 37 years considered here (Fig. 11c; Table 2). Besides, the WWV in western Pacific was significantly negative during Mar(0)–Jul(0) in 2015 (Fig. 11d). Apparently, those WWV signals alone were not sufficient conditions for this extremely strong El Niño. However, the formation of a strong El Niño could be promoted by the extremely warm SSTA in the SNP (1.0°C; ranking first) in 2015, larger than 2 times its standard deviation (std = 0.45°C).

Warm SSTAs in the SNP and SSP also helped other El Niño events come into being (e.g., the 1994 El Niño and the 1987 El Niño). Before these two El Niño events, both the basinwide WWV and the WWV in the western Pacific were negative at the leading time of Mar(0)–Jul(0) (Figs. 11c,d), an unfavorable precondition for El Niño events. However, the two moderate El Niños were formed under the background of positive SSTAs in both the SNP and SSP. Since the warm SSTAs in the Niño-3.4 region continuously maintained a high value as an

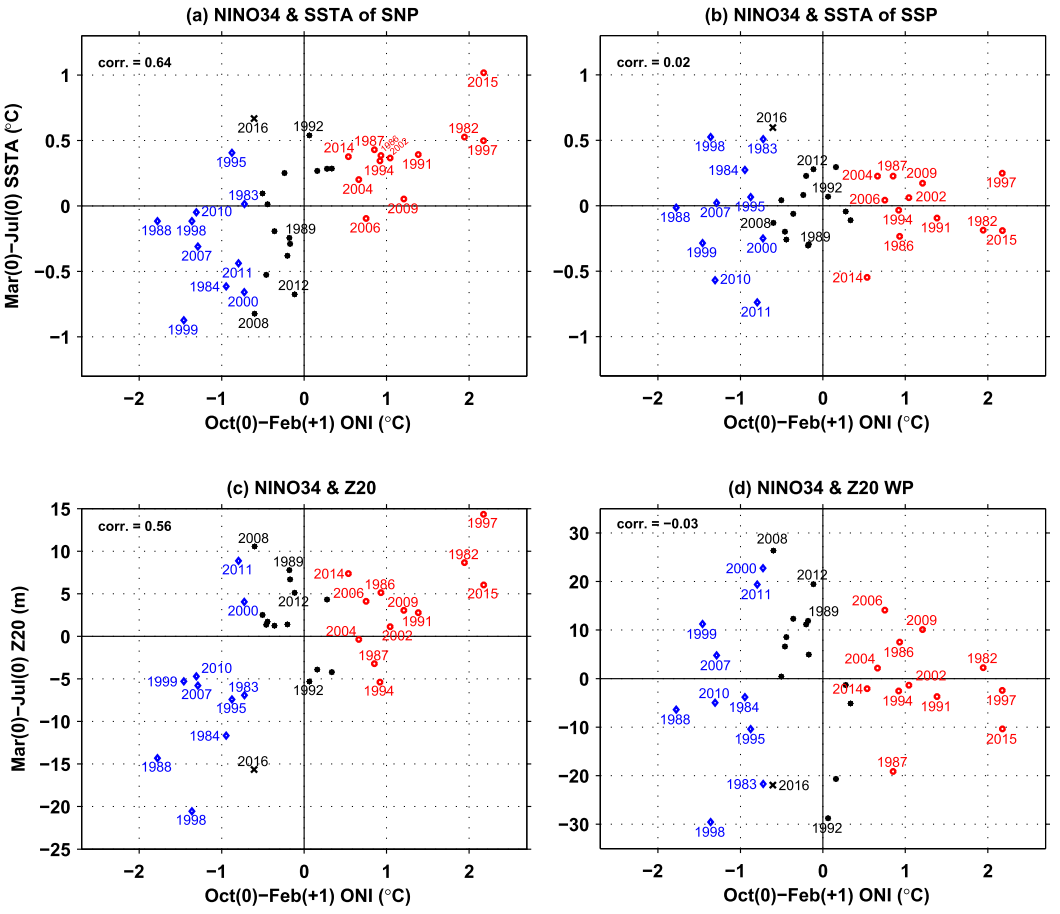

FIG. 11. The scatterplot of winter ONI against leading signals during spring–summer of (a) SSTAs in SNP (5°–15°N, 140°–170°W), (b) SSTAs in SSP (10°–20°S, 130°–90°W), (c) thermocline depth anomalies in the equatorial Pacific (5°N–5°S, 120°E–80°W), and (d) thermocline depth anomalies in the equatorial western Pacific (5°N–5°S, 120°E–180°). The Niño-3.4 index values during Oct(0)–Feb(+1) are plotted on the *x* axis, and values of other leading signals during Mar(0)–Jul(0) are plotted on the *y* axis. The years of El Niño, La Niña, and neutral events are displayed with red circles, blue rhombuses, and black dots, respectively. The year 2016 is displayed with a cross.

extension of the previous El Niño in 1986, it is hard to evaluate the contribution of SSTAs in the SNP and SSP to the formation of the 1987 El Niño. In contrast, there were not any apparent warming signals in the equatorial Pacific before the 1994 El Niño. Hence, it is easy to draw the conclusion that the warm SSTAs in subtropical Pacific boosted the 1994 El Niño (Su et al. 2014a).

In contrast, cold SSTAs in the subtropical Pacific can prevent an El Niño from developing sufficiently. In addition to the 2014 hindered El Niño, a false El Niño was announced in the boreal summer of 2012. Such similar features can also be found in the warming event in 2008, as discussed by Su et al. (2014b). All these three hindered warming events (2008, 2012, and 2014) share some common features (Fig. 11; Table 2), including the high warm WWV along the equatorial Pacific and the apparent cooling in subtropical Pacific. In fact, the transient warming event in 2008 once had an appealing precondition of the extreme high basinwide WWV (ranking second) and a high WWV in the western Pacific (ranking first). Anyway, in a cooling brought about by negative subtropical SSTAs from both the northern (−0.8°C) and southern (−0.1°C) Pacific, a diminished warming in the equatorial Pacific seemed quite inevitable.

The strength of leading negative basinwide WWV during 2016 ranked second among all the years in recent decades after 1980, falling just behind the strongest one during 1998 (Fig. 11c). At the same time, the high SNP SSTAs during 2016 ranked second, weaker than those of 2015 (Fig. 11a). From this aspect, it seems not so surprising to see that the 2016 La Niña was hindered from fully developing, as the SNP SSTAs were extra warm during the spring–summer season in 2016, which tended to induce anomalous westerlies near the equator. Typically, a strong El Niño event (e.g., 1982/83 and 1997/

TABLE 2. Some ENSO events associated with significant influences of the SSTAs in subtropical North Pacific (SNP SSTA; 5°–15°N, 140°–170°W) and subtropical South Pacific (SSP SSTA; 10°–20°S, 130°–90°W). The variables include the SSTAs in the Niño-3.4 region during Oct(0)–Feb(+1) (winter ONI; °C), the Z20 (m) averaged in the equatorial Pacific (EQ Z20; 5°N–5°S, 120°E–80°W), and the Z20 averaged in the equatorial western Pacific (WP Z20; 5°N–5°S, 120°E–180°). All the values are the mean over the period Mar(0)–Jul(0), except the winter ONI.

ENSO event	Winter ONI (°C)	SNP SSTA (°C)	SSP SSTA (°C)	EQ Z20 (m)	WP Z20 (m)
2015 super El Niño	2.2	1.0	−0.2	6.0	−10.4
1994 El Niño	0.9	0.3	0.0	−5.4	−2.6
1987 El Niño	0.9	0.4	0.2	−3.2	−19.1
2014 hindered El Niño	0.5	0.4	−0.6	7.4	−2.1
2012 hindered El Niño	−0.1	−0.7	0.3	5.1	19.4
2008 transient El Niño	−0.6	−0.8	−0.1	10.6	26.3
2016 hindered La Niña	−0.6	0.7	0.6	−15.7	−21.9
2011 La Niña	−0.8	−0.4	−0.7	8.9	19.4
1989 neutral ENSO event	−0.2	−0.2	−0.3	7.8	11.9
1992 neutral ENSO event	0.1	0.5	0.1	−5.3	−28.7

98) tends to decay quickly and be followed by a long-lasting La Niña event, which usually has an elongated lifetime of about two years (e.g., 1983 La Niña and 1984/85 La Niña in succession, and 1998–2000 La Niña). However, the weak cold status (about −0.6°C) after the 2015 super El Niño lasted only about five months and rebounded back to above −0.5°C after March 2017, when the warm SSTAs in the subtropical Pacific exerted an essential influence in hindering the cooling tendency at the equator. Significant negative SSTAs can be found in the subtropical Pacific during the decaying phase of other strong El Niño events (Figs. 11a,b). Hence, the formation of a full-fledged La Niña event may require negative SSTAs in the subtropical Pacific as a prerequisite.

Another compelling example is the formation of the 2011/12 La Niña. After the decaying phase of the previous 2010/11 La Niña, the equatorial Pacific was apparently warm (Fig. 11c), superficially indicating that no La Niña would arise in the following seasons. However, the decaying 2010/11 La Niña finally evolved into another La Niña event, partially due to the cold SSTAs in the subtropical Pacific in both hemispheres. Zheng et al. (2015) speculated that the subsurface intrusion of subtropical cold waters into the equatorial Pacific could play an important role in the formation of the 2011/12 La Niña, an oceanic process similar to the formation of the 1994 El Niño formation (Su et al. 2014a).

Interestingly, the influences of SSTAs in the SNP and SSP can also be detected in some neutral ENSO events. For example, significant positive basinwide WWV can be found in the spring–summer of 1989 (ranking fifth), and negative WWV signals persisted in the western Pacific in 1992 (ranking second; just weaker than that in 1998) (Figs. 11c,d; Table 2). However, the signs of SSTAs in the SNP and SSP were opposite those of the WWV. As a result, no El Niño or La Niña event formed in these two years.

The present analyses have shown that the subtropical Pacific either can assist El Niño or La Niña event growth without initial favorable subsurface temperature anomalies in the equatorial Pacific (e.g., 1994 El Niño, 2011 La Niña, and 2015 El Niño) or can hinder them from developing as expected (e.g., 2012 warming, 2014 warming, and 2016 cold events). In general, the warming SSTAs in the subtropical Pacific tend to weaken the trade winds, leading to anomalous westerlies along the equatorial region that favor the formation of El Niño events and hinder growth of La Niña events. On the other hand, in the case of cooling SSTAs in the subtropical Pacific, the trade winds tend to be enhanced and then lead to anomalous easterlies along the equatorial region, which would favor the formation of La Niña events and hinder growth of El Niño events. The subtropical SSTAs both can affect the developing phase of an ENSO event and also can influence its decaying phase. Two examples are the transformation from the decaying 2010/11 La Niña into another (2011/12) La Niña or the transformation from 2015 super El Niño to a neutral status in 2016. The hindered La Niña in 2016 can be considered a ''negative image'' of the aborted El Niño in 2012, both of which were hindered from developing by unfavorable trade wind anomalies.

7. The decadal changes of the effects of subtropical Pacific

During most of the 1980s and 1990s, the subtropical northeastern Pacific was occupied by positive SSTAs (Fig. 12a), associated with the positive phase of PDO. After the 1997 super El Niño, the SSTAs in the subtropical Pacific changed to a negative status, as the PDO evolved

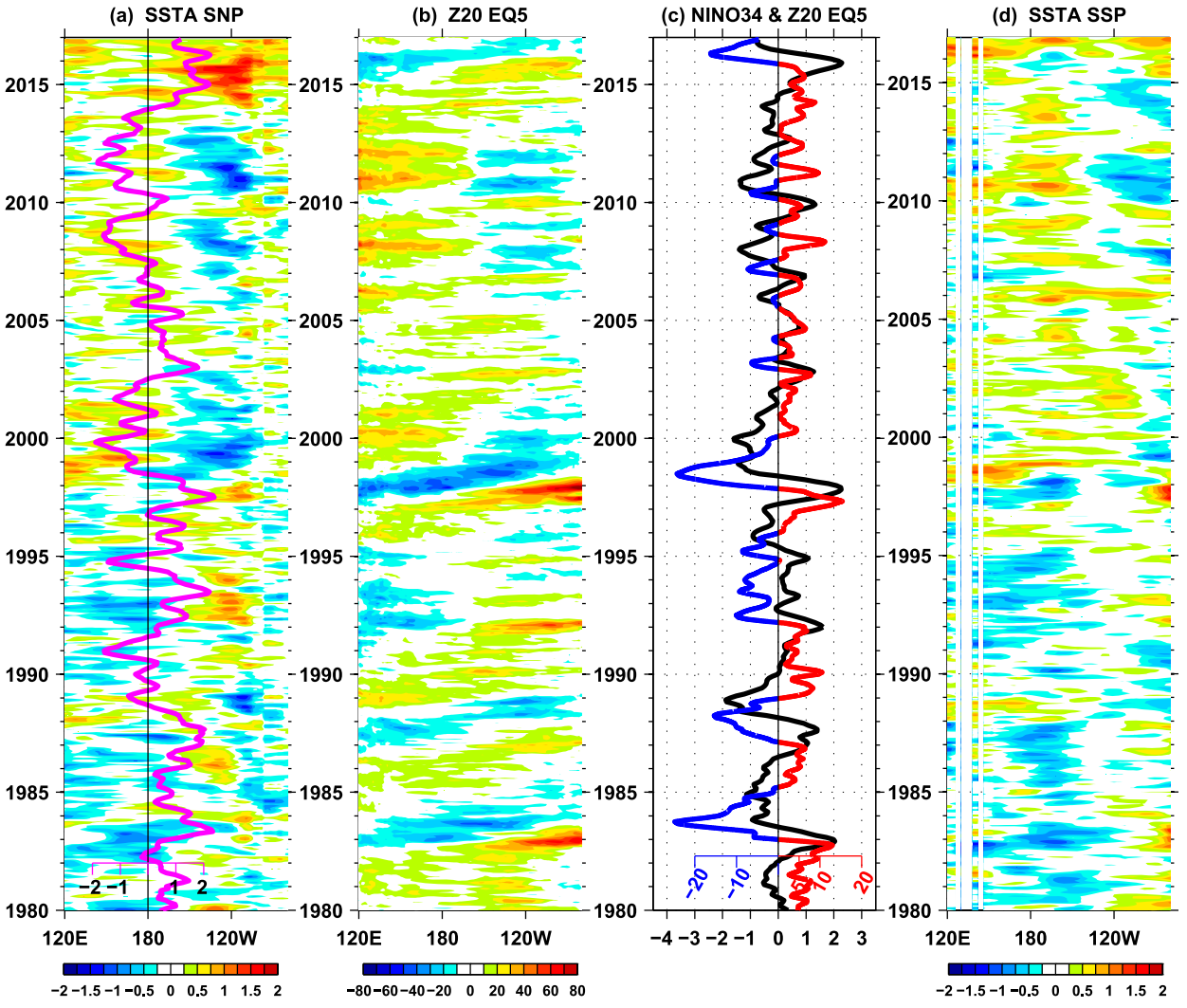

FIG. 12. (a) SSTA (shading, with intervals of 0.25°C) along the SNP (within 5°–15°N). (b) Z20 (shading, with intervals of 10 m) along the equator (within 5°N–5°S). (c) SSTA time series (black line; °C) averaged in the Niño-3.4 region and Z20 (red and blue line, multiplied by 0.1; m;) averaged in the equatorial Pacific (5°N–5°S, 120°E–180°). (d) SSTA evolution (shading, with intervals of 0.25°C) along the subtropical South Pacific (within 10°–20°S). The PDO index is plotted in (a) with a magenta line. The Niño-3.4 and Z20 (PDO) index time series are smoothed with a 3-month (5 month) moving average.

into its negative phase. During the period 1980–97, the positive WWV in the equatorial Pacific was an efficient indicator for the generation of El Niño events, while negative WWV indicated La Niña events. All El Niño events in 1982, 1986, and 1997 had similar initial conditions: warm subsurface temperature anomalies in the equatorial Pacific. However, there were no such subsurface warming anomalies before the occurrence of the 1994 El Niño, and its formation was primarily caused by the positive SSTAs in the subtropical Pacific (Su et al. 2014a).

Subsurface temperature anomalies in the equatorial Pacific were no longer an accurate predictor after 2000 (McPhaden 2012), which can also be inferred by the degraded predictive skills for ENSO during the same period (Barnston et al. 2012). The subsurface temperature anomalies maintained a warming status during most of 2000–14 (Fig. 12c). Although subsurface temperature anomalies in the equatorial Pacific had already reached a very high positive value several times (e.g., 2000, 2008, and 2011), no El Niño events were formed following such warm initial conditions. The hindered warming events after 2000 were generally related to the negative SSTAs in the subtropical Pacific, particularly in the subtropical northeastern Pacific, which prevented the equatorial westerlies from strengthening and maintaining. As the PDO returned to its positive phase around 2014, the subtropical eastern Pacific was

occupied by positive SSTAs after 2014 (Fig. 12a). Such warm SSTAs in subtropical regions favored the 2015 super El Niño; even the initial WWV in the equatorial Pacific only had a moderate value. This observed fact further supports the hypothesis that SSTAs in the subtropical Pacific exert a crucial influence on ENSO and its evolution.

It has been argued that ENSO has displayed more diversity since 2000, which was attributed to global warming (e.g., Yeh et al. 2009; Cai et al. 2014; Chen et al. 2015b) or the PDO (e.g., McPhaden et al. 2011; Capotondi et al. 2015). It was also argued that the ENSO diversity might result from westerly wind events (e.g., Hu et al. 2014; D. Chen et al. 2015; Fedorov et al. 2015). Here, we emphasize that the SSTAs in the subtropical Pacific may play a major role in the formation of El Niño and La Niña events. Because the subtropical Pacific can capture the major influence of the PDO variability (Fig. 12a), the contribution of the subtropical Pacific SSTAs also represents a PDO influence on ENSO. Based on the present analysis, we conclude that the diversity in ENSO can be explained mostly by the SSTAs in the subtropical Pacific.

In fact, the background of ongoing global warming never stopped after the 1970s, even during the so-called hiatus period after 1999 (Su et al. 2017). Therefore, it is hard to say that global warming is the basic reason for ENSO evolution from its classical features before 2000 to its unexpected diversity in recent decades. Such changes in ENSO diversity around 2000 may be related with the phase changes of the PDO, which can be well captured by the SSTAs in the subtropical Pacific. Furthermore, the 2015 super El Niño occurred during a positive phase of the PDO, with an index of approximately 2, which is the same as the 1982 and 1997 super El Niño events. However, the initial subsurface warming status between the 2015 El Niño and the two other super El Niños showed an apparent difference, demonstrating that the SSTAs in the subtropical Pacific may be crucial for El Niño formation.

8. Discussion

It can be concluded that the SSTAs in the subtropical Pacific can play an important role in the formation both of El Niño and La Niña events as an additional influence beyond the two generally known impacts: the warming state in the equatorial Pacific and the WWEs. In some special cases (e.g., 1994/95 El Niño, 2011/12 La Niña, and 2015/16 El Niño), the anomalous temperature in the subtropical Pacific may have played a leading role in the formation of El Niño and La Niña events; the upper oceanic state in the equatorial Pacific prior to these events was not favorable to their development. As the anomalous westerlies in the western-central equatorial Pacific can be driven by changes in the trade winds, the SSTAs in the subtropical Pacific may be an independent factor influencing ENSO evolution. Besides, the oceanic temperature anomalies in the subtropical Pacific can be transported equatorially by the subsurface oceanic currents, where they exert a potentially important impact for ENSO evolution (Su et al. 2010; Zheng et al. 2015).

Here, we emphasize that weakened trade winds (i.e., southwesterly/northwesterly anomalies in the off-equatorial region) can reinforce the westerly anomalies in the western-central equatorial Pacific. Because anomalous trade winds, which are coupled with subtropical SSTAs, can persist for several months, the favored westerly anomalies along the equator can be sustained for a longer time compared to the case without weakened trade winds. The long-lasting westerly anomalies play a crucial role in the growth of the SSTAs in the central-eastern equatorial Pacific. Because the WWEs in the western Pacific, as well as the equatorial oceanic free Kelvin waves, typically occur on intraseasonal time scales (e.g., Seiki and Takayabu 2007; Kessler et al. 1995; Chen et al. 2017), an extension of such WWEs from approximately one or two months to a longer time period is really required for the initial condition of oceanic warming to grow into a mature El Niño event. The maintenance and enhancement of such WWEs is influenced by trade wind changes, which can be induced on a time scale of several months, by the self-maintaining SSTAs in the subtropical Pacific. Such long-lasting maintenance of WWEs is definitely a crucial factor for ENSO formation, particularly during the ENSO developing phase when the SSTAs in the Niño-3.4 region have not been warmed enough to set up a positive Bjerknes feedback. Furthermore, the potential Bjerknes feedback between the oceanic warming or cooling status and atmospheric responses may be broken by those wind anomalies caused by the subtropical SSTAs, even the Niño-3.4 SSTAs that had already reached an El Niño/La Niña status from the oceanic point of view (e.g., 2014 El Niño and 2016 La Niña).

Considering the difficulties arising in ENSO prediction in recent years, improving the present ENSO prediction models is urgently needed. Achieving the necessary improvements requires a comprehensive and more precise investigation of the role played by the subtropical Pacific in ENSO formation. Furthermore, ENSO events have displayed greater diversity in recent decades in the context of global warming and the PDO. Explaining this diversity may depend on observations and investigations of the subtropical North and South

Pacific, which exert different effects on the formation of El Niño events.

Acknowledgments. Comments from the three anonymous reviewers were helpful to improving the paper. This work is supported by the National Key R&D Program of China (2016YFA0600602), the Special Fund for Public Welfare Industry (GYHY201506013), and the National Natural Science Foundation of China (41776039, 41475057, and 41376020).

REFERENCES

Alexander, M. A., I. Bladé, M. Newman, J. R. Lanzante, N.-C. Lau, and J. D. Scott, 2002: The atmospheric bridge: The influence of ENSO teleconnections on air–sea interaction over the global oceans. *J. Climate*, **15**, 2205–2231, https://doi.org/10.1175/1520-0442(2002)015<2205:TABTIO>2.0.CO;2.

Ashok, K., S. K. Behera, S. A. Rao, H. Weng, and T. Yamagata, 2007: El Niño Modoki and its possible teleconnection. *J. Geophys. Res.*, **112**, C11007, https://doi.org/10.1029/2006JC003798.

Barnston, A. G., M. K. Tippett, M. L. L'Heureux, S. Li, and D. G. DeWitt, 2012: Skill of real-time seasonal ENSO model predictions during 2002–11: Is our capability increasing? *Bull. Amer. Meteor. Soc.*, **93**, 631–651, https://doi.org/10.1175/BAMS-D-11-00111.1.

Cai, W., and Coauthors, 2014: Increasing frequency of extreme El Niño events due to greenhouse warming. *Nat. Climate Change*, **4**, 111–116, https://doi.org/10.1038/nclimate2100.

Capotondi, A., and Coauthors, 2015: Understanding ENSO diversity. *Bull. Amer. Meteor. Soc.*, **96**, 921–938, https://doi.org/10.1175/BAMS-D-13-00117.1.

Chen, D., and Coauthors, 2015: Strong influence of westerly wind bursts on El Niño diversity. *Nat. Geosci.*, **8**, 339–345, https://doi.org/10.1038/ngeo2399.

Chen, L., T. Li, and Y. Yu, 2015: Causes of strengthening and weakening of ENSO amplitude under global warming in four CMIP5 models. *J. Climate*, **28**, 3250–3274, https://doi.org/10.1175/JCLI-D-14-00439.1.

——, ——, S. K. Behera, and T. Doi, 2016: Distinctive precursory air–sea signals between regular and super El Niños. *Adv. Atmos. Sci.*, **33**, 996–1004, https://doi.org/10.1007/s00376-016-5250-8.

——, ——, B. Wang, and L. Wang, 2017: Formation mechanism for 2015/16 super El Niño. *Sci. Rep.*, **7**, 2975, https://doi.org/10.1038/s41598-017-02926-3.

Dee, D., and Coauthors, 2011: The ERA-Interim reanalysis: Configuration and performance of the data assimilation system. *Quart. J. Roy. Meteor. Soc.*, **137**, 553–597, https://doi.org/10.1002/qj.828.

Di Lorenzo, E., and N. Mantua, 2016: Multi-year persistence of the 2014/15 North Pacific marine heatwave. *Nat. Climate Change*, **6**, 1042–1047, https://doi.org/10.1038/nclimate3082.

Fedorov, A. V., S. Hu, M. Lengaigne, and E. Guilyardi, 2015: The impact of westerly wind bursts and ocean initial state on the development and diversity of El Niño events. *Climate Dyn.*, **44**, 1381–1401, https://doi.org/10.1007/s00382-014-2126-4.

Gill, A. E., 1980: Some simple solutions for heat-induced tropical circulation. *Quart. J. Roy. Meteor. Soc.*, **106**, 447–462, https://doi.org/10.1002/qj.49710644905.

Graham, N. E., and T. P. Barnett, 1987: Sea surface temperature, surface wind divergence, and convection over tropical oceans. *Science*, **238**, 657–659, https://doi.org/10.1126/science.238.4827.657.

Hong, C.-C., H.-H. Hsu, W.-L. Tseng, M.-Y. Lee, C.-H. Chow, and L.-C. Jiang, 2017: Extratropical forcing triggered the 2015 Madden–Julian Oscillation–El Niño event. *Sci. Rep.*, **7**, 46692, https://doi.org/10.1038/srep46692.

Hu, S., and A. V. Fedorov, 2016: Exceptionally strong easterly wind burst stalling El Niño of 2014. *Proc. Natl. Acad. Sci. USA*, **113**, 2005–2010, https://doi.org/10.1073/pnas.1514182113.

——, and ——, 2018: The extreme El Niño of 2015–2016: The role of westerly and easterly wind bursts, and preconditioning by the failed 2014 event. *Climate Dyn.*, https://doi.org/10.1007/s00382-017-3531-2, in press.

——, ——, M. Lengaigne, and E. Guilyardi, 2014: The impact of westerly wind bursts on the diversity and predictability of El Niño events: An ocean energetics perspective. *Geophys. Res. Lett.*, **41**, 4654–4663, https://doi.org/10.1002/2014GL059573.

Huang, B., and Coauthors, 2015: Extended Reconstructed Sea Surface Temperature version 4 (ERSST.v4). Part I: Upgrades and intercomparisons. *J. Climate*, **28**, 911–930, https://doi.org/10.1175/JCLI-D-14-00006.1.

Huang, R., R. Zhang, and B. Yan, 2001: Dynamical effect of the zonal wind anomalies over the tropical western Pacific on ENSO cycles. *Sci. China*, **44D**, 1089–1098, https://doi.org/10.1007/BF02906865.

Kessler, W. S., M. J. McPhaden, and K. M. Weickmann, 1995: Forcing of intraseasonal Kelvin waves in the equatorial Pacific. *J. Geophys. Res.*, **100**, 10 613–10 631, https://doi.org/10.1029/95JC00382.

Latif, M., and Coauthors, 1998: A review of the predictability and prediction of ENSO. *J. Geophys. Res.*, **103**, 14 375–14 393, https://doi.org/10.1029/97JC03413.

Luther, D. S., D. E. Harrison, and R. A. Knox, 1983: Zonal winds in the central equatorial Pacific and El Niño. *Science*, **222**, 327–330, https://doi.org/10.1126/science.222.4621.327.

McPhaden, M. J., 2012: A 21st century shift in the relationship between ENSO SST and warm water volume anomalies. *Geophys. Res. Lett.*, **39**, L09706, https://doi.org/10.1029/2012GL051826.

——, and J. Picaut, 1990: El Niño–Southern Oscillation displacements of the western equatorial Pacific warm pool. *Science*, **250**, 1385–1388, https://doi.org/10.1126/science.250.4986.1385.

——, F. Bahr, Y. Du Penhoat, E. Firing, S. P. Hayes, P. P. Niiler, P. L. Richardson, and J. M. Toole, 1992: The response of the western equatorial Pacific Ocean to westerly wind bursts during November 1989 to January 1990. *J. Geophys. Res.*, **97**, 14 289–14 303, https://doi.org/10.1029/92JC01197.

——, and Coauthors, 1998: The Tropical Ocean–Global Atmosphere observing system: A decade of progress. *J. Geophys. Res.*, **103**, 14 169–14 240, https://doi.org/10.1029/97JC02906.

——, T. Lee, and D. McClurg, 2011: El Niño and its relationship to changing background conditions in the tropical Pacific Ocean. *Geophys. Res. Lett.*, **38**, L15709, https://doi.org/10.1029/2011GL048275.

Meinen, C. S., and M. J. McPhaden, 2000: Observations of warm water volume changes in the equatorial Pacific and their relationship to El Niño and La Niña. *J. Climate*, **13**, 3551–3559, https://doi.org/10.1175/1520-0442(2000)013<3551:OOWWVC>2.0.CO;2.

Menkes, C. E., M. Lengaigne, J. Vialard, M. Puy, P. Marchesiello, S. Cravatte, and G. Cambon, 2014: About the role of westerly

wind events in the possible development of an El Niño in 2014. *Geophys. Res. Lett.*, **41**, 6476–6483, https://doi.org/10.1002/2014GL061186.

Miller, L., R. E. Cheney, and B. C. Douglas, 1988: GEOSAT altimeter observations of Kelvin waves and the 1986-87 El Niño. *Science*, **239**, 52–54, https://doi.org/10.1126/science.239.4835.52.

Min, Q., J. Su, R. Zhang, and X. Rong, 2015: What hindered the El Niño pattern in 2014? *Geophys. Res. Lett.*, **42**, 6762–6770, https://doi.org/10.1002/2015GL064899.

——, ——, and ——, 2017: Impact of the South and North Pacific meridional modes on the El Niño–Southern Oscillation: Observational analysis and comparison. *J. Climate*, **30**, 1705–1720, https://doi.org/10.1175/JCLI-D-16-0063.1.

Paek, H., J.-Y. Yu, and C. Qian, 2017: Why were the 2015/2016 and 1997/1998 extreme El Niños different? *Geophys. Res. Lett.*, **44**, 1848–1856, https://doi.org/10.1002/2016GL071515.

Rayner, N. A., D. E. Parker, E. B. Horton, C. K. Folland, L. V. Alexander, D. P. Rowell, E. C. Kent, and A. Kaplan, 2003: Global analyses of sea surface temperature, sea ice, and night marine air temperature since the late nineteenth century. *J. Geophys. Res.*, **108**, 4407, https://doi.org/10.1029/2002JD002670.

Reynolds, R. W., N. A. Rayner, T. M. Smith, D. C. Stokes, and W. Wang, 2002: An improved in situ and satellite SST analysis for climate. *J. Climate*, **15**, 1609–1625, https://doi.org/10.1175/1520-0442(2002)015<1609:AIISAS>2.0.CO;2.

Roeckner, E., and Coauthors, 2003: The atmospheric general circulation model ECHAM5. Part I: Model description. Max-Planck-Institut für Meteorologie Tech. Rep. 349, 140 pp., http://mms.dkrz.de/pdf/klimadaten/service_support/documents/mpi_report_349.pdf.

Saha, S., and Coauthors, 2006: The NCEP Climate Forecast System. *J. Climate*, **19**, 3483–3517, https://doi.org/10.1175/JCLI3812.1.

Seiki, A., and Y. N. Takayabu, 2007: Westerly wind bursts and their relationship with intraseasonal variations and ENSO. Part I: Statistics. *Mon. Wea. Rev.*, **135**, 3325–3345, https://doi.org/10.1175/MWR3477.1.

Su, J., R. Zhang, T. Li, X. Rong, J.-S. Kug, and C.-C. Hong, 2010: Causes of the El Niño and La Niña amplitude asymmetry in the equatorial eastern Pacific. *J. Climate*, **23**, 605–617, https://doi.org/10.1175/2009JCLI2894.1.

——, T. Li, and R. Zhang, 2014a: The initiation and developing mechanisms of central Pacific El Niños. *J. Climate*, **27**, 4473–4485, https://doi.org/10.1175/JCLI-D-13-00640.1.

——, B. Xiang, B. Wang, and T. Li, 2014b: Abrupt termination of the 2012 Pacific warming and its implication on ENSO prediction. *Geophys. Res. Lett.*, **41**, 9058–9064, https://doi.org/10.1002/2014GL062380.

——, R. Zhang, and H. Wang, 2017: Consecutive record-breaking high temperatures marked the handover from hiatus to accelerated warming. *Sci. Rep.*, **7**, 43735, https://doi.org/10.1038/srep43735.

Suarez, M. J., and P. S. Schopf, 1988: A delayed action oscillator for ENSO. *J. Atmos. Sci.*, **45**, 3283–3287, https://doi.org/10.1175/1520-0469(1988)045<3283:ADAOFE>2.0.CO;2.

Vimont, D. J., J. M. Wallace, and D. S. Battisti, 2003: The seasonal footprinting mechanism in the Pacific: Implications for ENSO. *J. Climate*, **16**, 2668–2675, https://doi.org/10.1175/1520-0442(2003)016<2668:TSFMIT>2.0.CO;2.

Wu, Y.-K., L. Chen, C.-C. Hong, T. Li, C.-T. Chen, and L. Wang, 2018: Role of the meridional dipole of SSTA and associated cross-equatorial flow in the tropical eastern Pacific in terminating the 2014 El Niño development. *Climate Dyn.*, https://doi.org/10.1007/s00382-017-3710-1, in press.

Wyrtki, K., 1975: El Niño—The dynamic response of the equatorial Pacific Ocean to atmospheric forcing. *J. Phys. Oceanogr.*, **5**, 572–584, https://doi.org/10.1175/1520-0485(1975)005<0572:ENTDRO>2.0.CO;2.

——, 1985: Water displacements in the Pacific and the genesis of El Niño cycles. *J. Geophys. Res.*, **90**, 7129–7132, https://doi.org/10.1029/JC090iC04p07129.

Xie, P., and P. A. Arkin, 1997: Global precipitation: A 17-year monthly analysis based on gauge observations, satellite estimates, and numerical model outputs. *Bull. Amer. Meteor. Soc.*, **78**, 2539–2558, https://doi.org/10.1175/1520-0477(1997)078<2539:GPAYMA>2.0.CO;2.

Xie, S.-P., and S. G. H. Philander, 1994: A coupled ocean–atmosphere model of relevance to the ITCZ in the eastern Pacific. *Tellus*, **46A**, 340–350, https://doi.org/10.3402/tellusa.v46i4.15484.

Xue, Y., and A. Kumar, 2017: Evolution of the 2015/16 El Niño and historical perspective since 1979. *Sci. China Earth Sci.*, **60**, 1572–1588, https://doi.org/10.1007/s11430-016-0106-9.

Yeh, S.-W., J.-S. Kug, B. Dewitte, M.-H. Kwon, B. P. Kirtman, and F.-F. Jin, 2009: El Niño in a changing climate. *Nature*, **461**, 511–514, https://doi.org/10.1038/nature08316.

Yu, J.-Y., H.-Y. Kao, and T. Lee, 2010: Subtropics-related interannual sea surface temperature variability in the central equatorial Pacific. *J. Climate*, **23**, 2869–2884, https://doi.org/10.1175/2010JCLI3171.1.

Zhang, H., A. Clement, and P. DiNezio, 2014: The South Pacific meridional mode: A mechanism for ENSO-like variability. *J. Climate*, **27**, 769–783, https://doi.org/10.1175/JCLI-D-13-00082.1.

Zheng, F., L. Feng, and J. Zhu, 2015: An incursion of off-equatorial subsurface cold water and its role in triggering the ''double dip'' La Niña event of 2011. *Adv. Atmos. Sci.*, **32**, 731–742, https://doi.org/10.1007/s00376-014-4080-9.

Zhu, J. S., A. Kumar, B. Huang, M. A. Balmaseda, Z.-Z. Hu, L. Marx, and J. L. Kinter III, 2016: The role of off-equatorial surface temperature anomalies in the 2014 El Niño prediction. *Sci. Rep.*, **6**, 19677, https://doi.org/10.1038/srep19677.